P3-39

Turbulence and Dust studies by Fast Camera Imaging Experiments in the TJ-II Stellarator

D. Carralero*, E. de la Cal, J. L. de Pablos, A. de Coninck, J.A. Alonso, C. Hidalgo, B. Ph. van Milligen and M.A. Pedrosa

Laboratorio Nacional de Fusión, EURATOM-CIEMAT, Madrid, Spain

Experimental studies of turbulence, plasma-wall interaction and dust by fast visible imaging in the TJ-II stellarator are presented. Low intensity phenomena were possible to be visualised by the installation of image intensifiers, allowing the direct observation of turbulent transport events in the scrape off layer (SOL). The analysis of plasma wall interaction by filtered imaging have shown that there is a change in the preferred interaction plasma-wall interaction area, going from a hard-core toroidally limited plasma to a poloidally locally limited one in the transition from ECRH to NBI heated plasmas. The observation of turbulent structures propagating poloidally at the plasma edge has shown enough periodicity to allow correlation between them with repetition rates around 10 kHz, as a quasi-coherent mode. Finally, dust generation and dynamics have been monitored by fast visible camera in boronized and lithiated vessel wall conditions during the first insertion of the limiter in the campaign.

PACS: 52.40.Hf, 52.55.Hc, 52.70.Kz, 52.35.Ra

JNM Keywords: Plasma-Materials Interaction, Impurities, Experimental Techniques

PSI-18 Keywords: TJ -II, Turbulence, Dust, Limiter, Lithium

**Corresponding author address:* Av. Complutense, 22. Madrid, Spain

**Corresponding author E-mail:* daniel.carralero@ciemat.es

Presenting author: Daniel Carralero Ortiz

I. Introduction

Several fast camera imaging experiments have been recently reported in different magnetic confinement devices [1-4]. Experiments carried out in the TJ-II stellarator have shown the impact of sheared flows on the geometrical characteristics of blobs [3] by means of continuous directional wavelet analysis. As well, several phenomena were observed in JET such as the macroscopic dust particle release from the wall during plasma disruptions and ELMs [4].

In this paper, experimental results from the fast visible fast camera upgrade in TJ-II stellarator are presented. After a brief description is provided of both the TJ-II stellarator and the experimental setup of the fast camera system (section II), three main issues are highlighted: the analysis of plasma wall interaction by spectroscopic imaging of atomic lines with interference filters (section III), the observation of quasi-coherent turbulent structures propagating poloidally at the plasma edge (section IV) and the ejection of dust into the plasma from the limiter operation (section V). Finally, some conclusions are stated and future work guidelines are proposed.

II. Experimental Setup

The TJ-II stellarator is a medium size machine currently under operation in CIEMAT, Madrid. Its main parameters are R=1.5 m., average minor radius of .22 m., B_T ~1T, $\iota(a)/2\pi$ ~1.6. Its heating systems include two ECRH gyrotrons of 300 kW (nominal power) and one NBI system with 1 MW of nominal power. Central electron temperatures up to 1 keV and densities of up to $4 \cdot 10^{-19}$ m^{-3} are achieved. Vacuum vessel is made out of stainless steel, with recycling processes enhanced by boronization and (during last campaign) lithiation. Plasma-wall interaction is usually localised at the

helical limiter (casing of the central solenoid), but can be changed at least partially when inserting the two mobile poloidal carbon limiters symmetrically spaced 180º [X]. Fast camera observation is performed through 2 different observation ports, looking at one of the limiters. One of these ports is tangential, and allows the observation line of sight to be almost perpendicular to the poloidal symmetry plane of the limiter (with less than 5º error), thus parallel to local field lines. The other view port is located in the poloidal plane of the limiter (slightly over it) and provides a close radial view of it.

The fast camera employed at TJ-II is a Photron APX based in CMOS technology capable of taking up to 250 kHz sampling rate videos. The Hamamatsu C9548 intensifier unit employed (a two stage device with a first Gen II coupled to a Gen I tube), has a high-speed gated system, capable of 100 kHz operation, with a maximum quantum efficiency of 15% (at 400 nm) and a resolution of 50 lp/mm. With this intensifier signal level can be effectively increased up to two orders of magnitude, allowing fast camera recording even at high rates in which no lighting phenomena were observable without it. The camera is placed on an optical bench, some meters away from TJ-II to avoid magnetic interactions. Optical coupling with the objective placed in the view-ports is realized via coherent fibre bundles and relay lenses. Narrow bandwidth interference filters (1 nm FWHM) can be placed before the objective in order to make spectroscopic visualisation of atomic lines. In that way specific emission lines are selected, thus discriminating the observed physical phenomena.

III. Poloidal Asymmetries in Plasma Surface Interaction Studies: role of ECRH and NBI heating

Spectroscopic two dimensional imaging using a lithium interference filter (centred at 670 nm) in a lithium-coated machine as TJ-II [5] allows the observation of plasma-wall interaction evolution as a function of plasma parameters and configuration. This is due to the fact that the Lithium atomic emission is proportional only to the lithium density and the electron density (there is nearly no electron temperature dependency) and its interpretation is more simple than that of H_α emission (different precursors and electron temperature dependency especially bellow 30 eV). The neutral lithium density, at least in front of limiters, is due to plasma sputtering and therefore proportional to the plasma out-flux. Plasma-wall interaction evolution during ECRH and NBI heating, with plasma density ramping and limiter insertion was investigated with image intensified videos taken with the lithium atomic line filter.

With the above mentioned experimental setup, several films were taken from the tangential port during an ECH and NBI operation day. In it, 600 kW of nominal ECH power and 1.5 MW of nominal NBI power were injected into the plasma, separated by some 40 ms. This generated a first ECH-like plasma reaching densities between 0.5-$1x10^{19}$ m^{-3}, followed by a density ramp (after the start of neutral injection) surpassing $3x10^{19}$ m^{-3}. The optical stage was set to observe both the limiter and the vessel walls, including the encased central solenoid. This central solenoid (in the following, the hard core) acts as a natural toroidal limiter for the plasma when poloidal limiters are retired. Relation between the radial position of the limiter and the recycling role of both devices has already been studied in ECH phase by means of a set of H-α detectors [6]. Now, NBI and ECH phases comparison is possible, as well as a more detailed observation of the geometric distribution of the recycling processes, thanks to the bidimensional vision provided by the intensified-fast-camera.

For this experiment, moderate sampling rates are employed (up to 17.5 kHz) in order to retain a broad observation area. Sequences are taken for several limiter positions, with distances to the Last Closed Flux Surface (LCFS) ranging from 5 to 20 mm. Figure (1) shows 4 snapshots selected in plasmas in which the limiter was located 10 mm out of the LCFS. In it, two main interaction areas can be observed, corresponding to the limiter (bottom flat region) and the hardcore (upper round area). The four images correspond to low and high density ECH plasmas (a and b, respectively) and increasing density NBI ones (c and d). Two immediate conclusions can be stated, even by naked eye observation: First, interaction is greater during ECH phase, despite the lower density and suggesting an improved confinement in NBI phase. Second, there is a change in the "preferred" interaction area, going from a hard-core toroidally limited plasma to a poloidally locally limited one.

To quantify both effects, further analysis has been performed: averaged signals have been obtained representing the level of interaction in both regions by taking the mean value in two arbitrary areas (red squares in the figures). Figure 2 shows the profile of both signals in plasmas with the limiter at 10 mm out of the LCFS and their ratios for 5, 10 and 20 mm (limiter positions). First visual impressions are now quantified with limiter signal up to a 50% greater than hard core in NBI phase. As well, the increase of the interaction in the limiter can be easily measured as it is gradually introduced in the plasma. Interestingly, an increase in the ratio appears after NBI start in the 5 and 10 mm. discharges (20 mm. discharge can be considered as no limiter one here) after ms. 1080, following a corresponding lineal increase in the density.

Other interesting feature of the sequence is the observation of fluctuations in signal levels in both regions: During the whole film, brightness (i.e. sputtering) is irregular and appears to be dominated by fluctuating processes. This may suggest a relation with turbulent transport mechanisms. As can be seen in 2, this fluctuation appears both in limiter and hardcore and seems to be reduced during the improved confinement NBI phase. To reach deeper insight of these phenomena, both signals are correlated to determine the degree of relation between them. As figure 3 shows, there is little to no correlation in the ECH or early NBI phases, with a great increase in correlation corresponding with the confined density ramp. This lack of correlation followed by an NBI driven increase can be observed in the three limiter positions with little difference between them. Similar results are obtained when correlating local signals at different positions of the limiter area. All these evidence support the idea of an isotropic, well confined plasma with less particle losses produced by large scale phenomena rather than by local, non isotropic turbulent ones, which would be quite reduced during this phase.

IV. Perpendicular Dynamics: Quasi-periodic rotation

Turbulent phenomena have also been analyzed with the described intensified fast camera. The use of the image intensifier allowed the camera to reach 100 kHz sampling rates with the limiter placed 20 mm away from the separatrix, thus working in turbulent relevant time scales (in the order of 10 μs). Both radial and tangential camera views positions were been employed to study ECRH plasmas

From tangential position, line of sight is almost parallel to the magnetic field in the region over the limiter. As most of the received light is emitted from the neutrals returning to the plasma after the recycling, this image can be considered a narrow

toroidal section of the plasma corresponding to the region immediately over the limiter. Correspondingly, images show a bright area decaying radially towards the center of the plasma. However, when only fluctuations in the signal are considered (Figure 4), a group of structures emerges moving within a radial stripe in the poloidal direction. These blobs could be the section of toroidal filaments poloidally rotating around the center of the plasma through its edge.

There is much previous work on the study of this blobs in TJ-II [3],[4]. Besides, experiments conducted with probes [7] provide evidence of a radial electric field creating an ExB drift in this plasma region. As well, observations indicate a change in the sign of this electric field when a certain density (around 0.65 $x10^{19}$ m^3) is surpassed.

This change of perpendicular rotation can be seen in fast camera movies by the naked eye when images (with mean values removed) are observed: at low densities, blobs rotation is anticlockwise, changing its sense after critical density is surpassed. In between both situations, an unstable regime prevails in which both rotations alternate. To quantify this apparent movement, correlation of locally sampled signals is employed again: the signal levels of two poloidally separated points are considered along the whole discharge. After some basic smoothing, both signals are correlated. As figure 5 shows, both signals have a high degree of correlation with a short delay between them. This delay corresponds to the time a blob takes to travel between the sampling points, giving a direct measure of poloidal flux velocity. Furthermore, a clear direction change can be observed after the passage of the critical density (around 1042 ms), as well as a non defined region around it. It must be noticed that the effect seems stronger in the right side of the figure due to the higher signal levels corresponding to higher densities.

Measured velocities are around 3.5±2 $km \cdot s^{-1}$, which fit measurements performed with probes [7]. The correlation map shows as well a regular horizontal pattern which suggests a quite constant rotation pattern: filaments are not only rotating at the same velocity, but they also show enough periodicity to allow correlation between them with repetition rates around 10 kHz, as a quasi-coherent mode.

From the radial position, toroidally elongated structures can be seen moving in poloidal directions, providing a visual confirmation of the filament hypothesis. Unfortunately, the privileged interpretation of tangential port images is no longer applicable here, for received signals are now integrated along an equally lit area. Although this does not impede the observation of the filaments themselves, correlation analysis as the precedent are inconclusive and will require further processing.

V. Dust Observation

Another relevant feature of the fast imaging system is impurity ejection and dust observation: for this, tangential vision, middle frame rate (around 15 kHz) non intensified films were recorded. The limiter was observed during its first insertion in the plasma along the campaign, following a series of lithiation processes. With this setting, a great amount of flakes and dusty phenomena could be observed for a few discharges, decaying afterwards to normal operation standards.

In the sequences (Figure 6), many different processes can be observed, as well as a broad range of velocities. However, many emitting flakes remain floating around the limiter moving at relatively slow velocities (around some tens of $m \cdot s^{-1}$) making their tracking possible even at these low sampling frequencies. About the nature of the flakes,

although indirect measurements (such as bolometry) suggest a low Z nature (carbon and lithium), no spectroscopic analysis interferometry has been performed yet, and no obvious relation can be established between the emission of the flakes and their origin. It should be remembered that the dust particle emission is due to both, blackbody radiation of the plasma-heated particle and due to atomic line emission. Future intensified imaging experiments with carbon and lithium interference filters will be made to develop a method to obtain information on the macroscopic particle composition from the emission.

VI. Conclusions

In conclusion, intensified fast visible cameras are a powerful tool in the investigation of plasma-wall interaction, turbulence and dust generation and dynamics in fusion devices. TJ-II results have shown a change in the preferred plasma-wall interaction area depending on plasma conditions (heating and density), the observation of quasi-coherent turbulent structures propagating poloidally at the plasma edge and dust generation and dynamics have been monitored in the proximity of the poloidal limiter after lithium coating.

[1] S. Zweben et al., Nuclear Fusion 44 (2004) 134

[2] J. Terry et al., Phys Plasmas 44 (2003) 1739

[3] J.A. Alonso et al., Plasma Physics Control. Fusion 48 (2006) B465

[4] J.A. Alonso et al., 34th EPS conference (Warsaw, 2007)

[5] F.L. Tabarés et al, EPS-2008

[6] E. de la Cal et al, J. Nucl. Mat., 290, p.579-583, (2001)

[7] M. A. Pedrosa et al., Plasma Physics and Controlled Fusion 49 (2007) B303

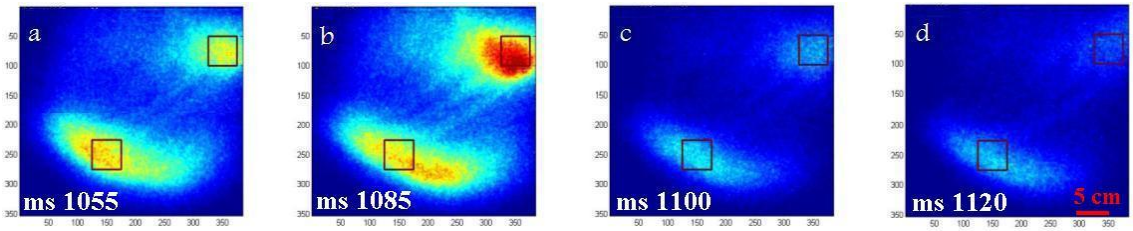

Figure 1: Discharge 18135. Interference filter imaging. Four snapshots of Lithium emission showing relative emission at limiter region (lower) and hard core region (upper). Limiter is 10 mm. away of the separatrix. Red squares show the sampling region.

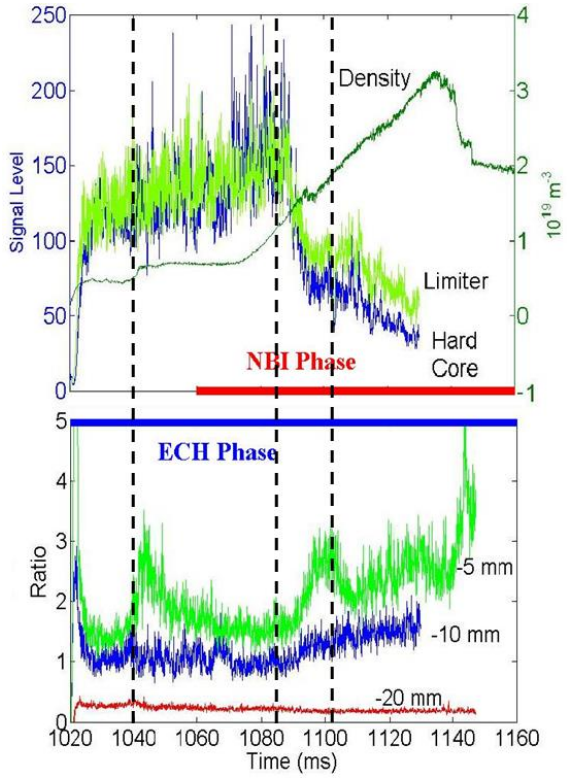

Figure 2: Discharges 18135(10mm),18137 (20 mm.) and 18152 (5mm). Signal sampling. Signal levels are shown at limiter and hard core for plasmas with the limiter located 10mm out of the LCFS (up) and

ratios between limiter and hardcore signals are shown for the three different limiter positions distances (down). Discharge density and heating phases are given as a reference.

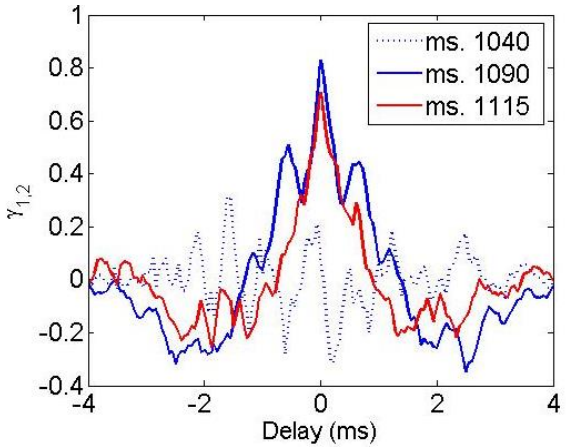

Figure 3: Signal Correlation. Limiter and hard core signals are correlated on the ms. time scale along the three times pointed in Figure 2, corresponding ECH phase, early and late NBI phases respectively. A sharp increase in the correlation can be noticed after the density increase.

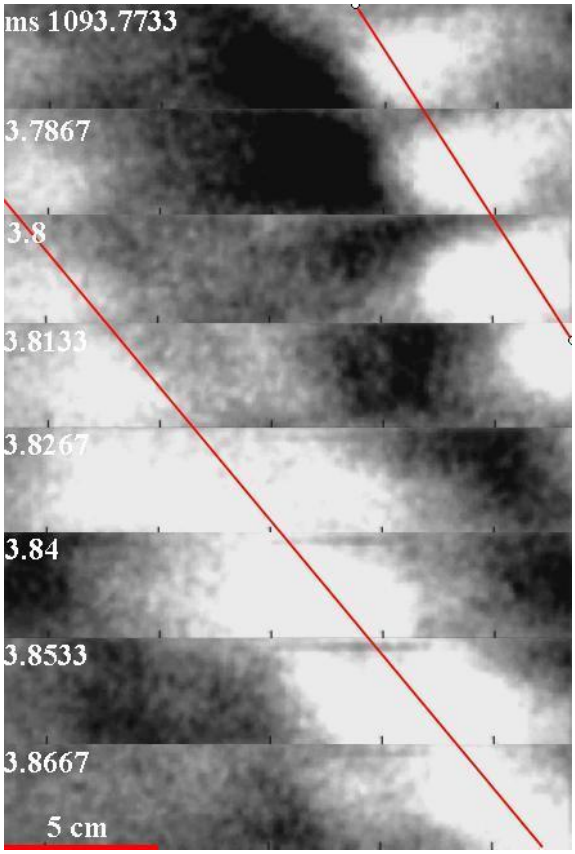

Figure 4: Discharge 17718. Tangential view. An array of successive snapshots of a high frame rate video is shown with their corresponding capture times. In it, blobs can be seen displacing poloidally along the images (separated by some 13 μs). Given the spatial reference, a velocity in the range of 5 $km \cdot s^{-1}$ can be calculated.

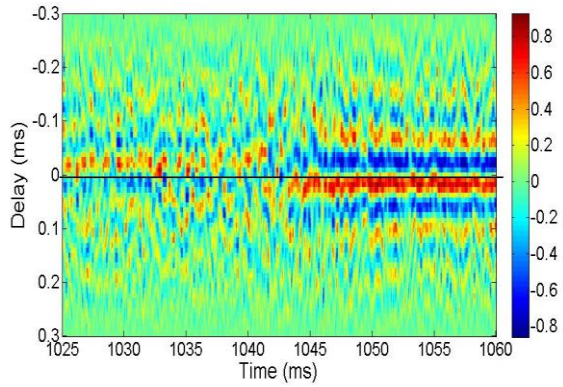

Figure 5: Discharge 18128. Change of rotation. Signals sampled in poloidally separated points of tangential view images (such as the ones in Figure 4) are correlated to determine the delay in the blob passage between them. Again, with spatial references, velocities of some km·s^{-1} are obtained. Notice the change in the sense of the rotation around ms. 1042 and the regular patter in the right hand side of the figure suggesting quasi-coherent modes.

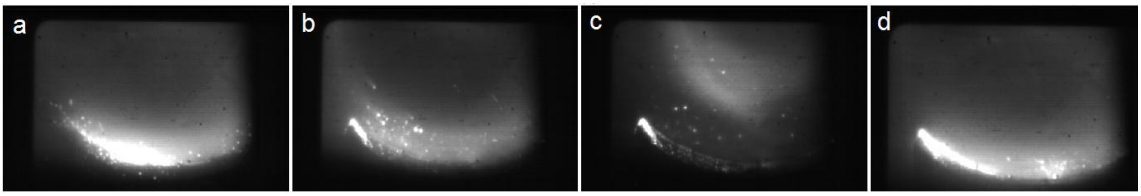

Figure 6: Discharge 17339. Dust observation. Several medium frame rate shots taken after the first insertion of the limiter during the campaign. From a-c, several moments of the discharge in which various shapes and sizes of flakes emit over the limiter (lower region). C shows last moments of the discharge, after cut-off (cold dense plasma remaining in the upper region). In d, an ejection event can be seen (bottom, right).